J|A|C|S ARTICLES

Published on Web 03/27/2009

Synthesis of J-Aggregating Dibenz[*a,j*]anthracene-Based Macrocycles

Julian M. W. Chan, Jonathan R. Tischler, Steve E. Kooi, Vladimir Bulović, and Timothy M. Swager*

Department of Chemistry and Department of Electrical Engineering and Computer Science, Massachusetts Institute of Technology, 77 Massachusetts Avenue, Cambridge, Massachusetts 02139

Received January 18, 2009; E-mail: tswager@mit.edu

Abstract: Several fluorescent macrocycles based on 1,3-butadiyne-bridged dibenz[*a,j*]anthracene subunits have been synthesized via a multistep route. The synthetic strategy involved the initial construction of a functionalized dibenz[*a,j*]anthracene building block, subsequent installation of free alkyne groups on one side of the polycyclic aromatic framework, and a final cyclization based on a modified Glaser coupling under high-dilution conditions. Photophysical studies on three conjugated macrocycles revealed the formation of J-aggregates in thin films, as well as in concentrated solid solutions (polyisobutylene matrix), with peak absorption and emission wavelength in the range of $\lambda = 460-480$ nm. The characteristic red-shifting of the J-aggregate features as compared to the monomer spectra, enhancement in absorption intensities, narrowed linewidths, and minimal Stokes shift values, were all observed. We demonstrate that improvements in spectral features can be brought about by annealing the films under a solvent-saturated atmosphere, where for the best films the luminescence quantum efficiency as high as 92% was measured. This class of macrocycles represents a new category of J-aggregates that due to their high peak oscillator strength and high luminescence efficiency have the potential to be utilized in a variety of optoelectronic devices.

Introduction

Shape-persistent macrocycles have received much attention in the field of materials science, particularly in the area of nanoscale architectures.[1] The first macrocycle featuring two unfunctionalized anthracenes linked by 1,3-butadiyne bridges was reported in 1960, but due to the lack of modern synthetic and characterization methods, the nature of the resulting material was not rigorously elucidated.[2] Following little interest in such systems over the next four decades, reports of anthrylene-ethynylene oligomers and macrocycles have surfaced in the past 5 years.[3] However, the molecular rigidity and lack of solubilizing groups resulted in the reported compounds having poor solubilities in common solvents. To create a class of molecules that could have potentially interesting photophysical and materials properties, we embarked on the design of conjugated macrocycles based on rigid dibenz[*a,j*]anthracene units bridged by butadiyne π-linkers. This was a logical choice since aryleneethynylene and 1,3-butadiyne linkages are frequently used in conjugated systems (e.g., polymers) for their ability to maintain rigidity and π-conjugation.[4] The polycyclic aromatic motifs are commonly seen in other areas of materials science, notably in the fields of discotic liquid crystals and graphitic materials.[5] By employing various modern synthetic transformations, it was possible to introduce numerous functionalities (e.g., side chains) into the structure to give better solubility and processability. In particular, bulky 4-alkoxyphenyl substituents located near the middle of the macrocycles serve several purposes: (1) as synthetic handles to allow for the facile electrophilic cyclizations[6] used to establish the dibenz[*a,j*]anthracene framework, (2) as solubilizing groups, and most importantly, (3) as a source of steric hindrance to bring about twisting of the π-system. Such distortion of the rigid framework by steric bulk has been known to induce slipped stacking arrangements,[7] resulting in aggregate structures with unique optical properties. Similar slipped structures are also known in nature: for example, the arrangement of J-aggregated chlorophyll chromophores is crucial to the light-harvesting efficiency of

(1) (a) Sakamoto, J.; Schlüter, A. D. *Eur. J. Org. Chem.* **2007**, 2700–2712. (b) Zhang, W.; Moore, J. S. *Angew. Chem., Int. Ed.* **2006**, *45*, 4416–4439. (c) Kumar, S. *Chem. Soc. Rev.* **2006**, *35*, 83–109.

(2) Akiyama, S.; Misumi, S.; Nakagawa, M. *Bull. Chem. Soc. Jpn.* **1960**, *33*, 1293–1298.

(3) (a) Toyota, S.; Goichi, M.; Kotani, M. *Angew. Chem., Int. Ed.* **2004**, *43*, 2248–2251. (b) Toyota, S.; Kurokawa, M.; Araki, M.; Nakamura, K.; Iwanaga, T. *Org. Lett.* **2007**, *9*, 3655–3658. (c) Goichi, M.; Toyota, S. *Chem. Lett.* **2006**, *35*, 684–685. (d) Goichi, M.; Segawa, K.; Suzuki, S.; Toyota, S. *Synthesis* **2005**, *13*, 2116–2118. (e) Toyota, S.; Goichi, M.; Kotani, M.; Takezaki, M. *Bull. Chem. Soc. Jpn.* **2005**, *78*, 2214–2227. (f) Toyota, S.; Suzuki, S.; Goichi, M. *Chem.—Eur. J.* **2006**, *12*, 2482–2487.

(4) (a) Taylor, M. S.; Swager, T. M. *Angew. Chem., Int. Ed.* **2007**, *46*, 8480–8483. (b) Bunz, U. H. F. *Chem. Rev.* **2000**, *100*, 1605–1644. (c) Becker, K.; Lagoudakis, P. G.; Gaefke, G.; Höger, S.; Lupton, J. M. *Angew. Chem., Int. Ed.* **2007**, *46*, 1. (d) Marsden, J. A.; Haley, M. M. *J. Org. Chem.* **2005**, *70*, 10213–10226.

(5) (a) Grimsdale, A. C.; Wu, J.; Müllen, K. *Chem. Commun.* **2005**, 2197–2204. (b) Tyutyulkov, N.; Müllen, K.; Baumgarten, M.; Ivanova, A.; Tadjer, A. *Synth. Met.* **2003**, *139*, 99–107. (c) Simpson, C. D.; Brand, J. D.; Berresheim, A. J.; Przybilla, L.; Rader, H. J.; Müllen, K. *Chem.—Eur. J.* **2002**, *8*, 1424–1429. (d) Ito, S.; Wehmeier, M.; Brand, J. D.; Kubel, C.; Epsch, R.; Rabe, J. P.; Müllen, K. *Chem.—Eur. J.* **2000**, *6*, 4327–4342.

(6) (a) Zhang, X.; Larock, R. C. *J. Am. Chem. Soc.* **2005**, *127*, 12230–12231. (b) Yao, T.; Campo, M. A.; Larock, R. C. *J. Org. Chem.* **2005**, *70*, 3511–3517.

(7) (a) Würthner, F. *Chem. Commun.* **2004**, 1564–1579. (b) Würthner, F. *Pure Appl. Chem.* **2006**, *78*, 2341–2349.

Scheme 1. Synthesis of Macrocycles **6a** and **6b**

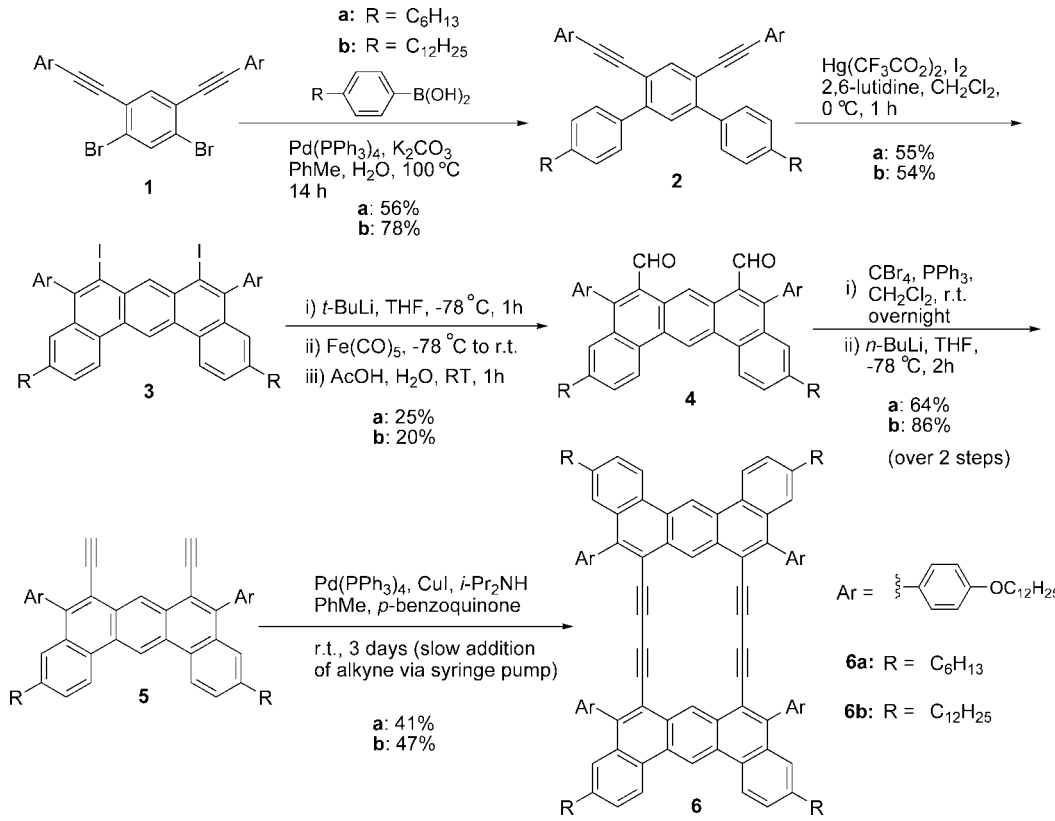

photosynthetic systems.[8] Using natural photosystems as a guide and inspiration, researchers have found ways to emulate this J-aggregate design in various porphyrins and perylene bisimides.[9] More recently, the laboratories of Frank Würthner have also successfully implemented the rational synthesis of several J-aggregated systems using supramolecular design principles.[10] Ever since their serendipitous discovery in 1936, J-aggregates have been of great theoretical interest because they display coherent, cooperative phenomena like superradiance and giant oscillator strength, a consequence of their electronic excitation being delocalized over several molecules.[11] Besides being theoretical curiosities, J-aggregates also have a myriad of practical applications, such as their use as organic photoconductors,[12] photopolymerization initiators,[13] and nonlinear optical devices,[14] as well as the emerging applications such as the recently demonstrated critically coupled resonators[15] and strongly QED coupled microcavity LEDs.[16]

Herein, we report the synthesis and characterization of a series of J-aggregating macrocycles based on functionalized dibenz[*a,j*]anthracene fragments linked at the 6- and 8- positions by a pair of 1,3-butadiyne bridges, in which the ring interior can be viewed as an octadehydro[18]annulene system. The results of their photophysical studies are also detailed.

Results and Discussion

Synthesis. Macrocycles **6a** and **6b** were prepared in six steps from the previously reported dibromide **1**[14] (Scheme 1). Subjecting the dibromide to a double Suzuki coupling with 4-alkylphenylboronic acids afforded terphenyl derivatives **2**, which were then converted to the required 6,8-diiododibenz[*a,j*]anthracenes via a double iodonium-induced electrophilic cyclization.[17,18] Numerous attempts to convert the diiodide to the bis-acetylene **5** via Sonogashira and Castro−Stephens reactions proved unsuccessful, instead resulting in complex,

(8) (a) Holzwarth, A. R.; Schaffner, K. *Photosynth. Res.* **1994**, *41*, 225–233. (b) McDermott, G.; Prince, S. M.; Freer, A. A.; Hawthornthwaite-Lawless, A. M.; Papiz, M. Z.; Cogdell, R. J.; Isaacs, N. W. *Nature (London)* **1995**, *374*, 517–521. (c) Pullerits, T.; Sundström, V. *Acc. Chem. Res.* **1996**, *29*, 381–389. (d) Balaban, T. S.; Tamiaki, H.; Holzwarth, A. R. *Top. Curr. Chem.* **2005**, *258*, 1–38.

(9) (a) Takahashi, R.; Kobuke, Y. *J. Am. Chem. Soc.* **2003**, *125*, 2372–2373. (b) Yamaguchi, T.; Kimura, T.; Matsuda, H.; Aida, T. *Angew. Chem., Int. Ed.* **2004**, *43*, 6350–6355. (c) Elemans, J. A. A. W.; van Hameren, R.; Nolte, R. J. M.; Rowan, A. E. *Adv. Mater.* **2006**, *18*, 1251–1266. (d) Wang, H.; Kaiser, T. E.; Uemura, S.; Würthner, F. *Chem. Commun.* **2008**, 1181–1183.

(10) (a) Kaiser, T. E.; Wang, H.; Stepanenko, V.; Würthner, F. *Angew. Chem., Int. Ed.* **2007**, *46*, 5541–5544. (b) Yagai, S.; Seki, T.; Karatsu, T.; Kitamura, A.; Würthner, F. *Angew. Chem., Int. Ed.* **2008**, *47*, 3367–3371. (c) Li, X.-Q.; Zhang, X.; Ghosh, S.; Würthner, F. *Chem.—Eur. J.* **2008**, *14*, 8074–8078. (d) Würthner, F.; Bauer, C.; Stepenenko, V.; Yagai, S. *Adv. Mater.* **2008**, *20*, 1695–1698.

(11) (a) Kobayashi, T., Ed. *J-Aggregates*; World Scientific: Singapore 1996. (b) Möbius, D. *Adv. Mater.* **1995**, *7*, 437–444.

(12) Borsenberger, P. M.; Chowdry, A.; Hoesterey, D. C.; Mey, W. *J. Appl. Phys.* **1978**, *44*, 5555–5564.

(13) Chatterjee, S.; Davis, P. D.; Gottschalk, P.; Kurz, M. E.; Sauerwein, B.; Yang, X.; Schuster, G. B. *J. Am. Chem. Soc.* **1990**, *112*, 6329–6338.

(14) (a) Wang, Y. *Chem. Phys. Lett.* **1986**, *126*, 209–214. (b) Wang, Y. *J. Opt. Soc. Am. B.* **1991**, *8*, 981–985. (c) Kobayashi, S. *Mol. Crys. Liq. Crys.* **1992**, *217*, 77–81.

(15) Tischler, J. R.; Bradley, M. S.; Bulović, V. *Opt. Lett.* **2006**, *31*, 2045–2047.

(16) (a) Tischler, J. R.; Bradley, M. S.; Bulović, V.; Song, J. H.; Nurmikko, A. *Phys. Rev. Lett.* **2005**, *95*, 036401. (b) Tischler, J. R.; Bradley, M. S.; Zhang, Q.; Atay, T.; Nurmikko, A.; Bulović, V. *Org. Electron.* **2007**, *8*, 94–113.

(17) Goldfinger, M. B.; Crawford, K. B.; Swager, T. M. *J. Am. Chem. Soc.* **1997**, *119*, 4578–4593.

(18) Goldfinger, M. B.; Khushrav, K. B.; Swager, T. M. *J. Org. Chem.* **1998**, *63*, 1676–1686.

Scheme 2. Synthesis of Macrocycle **12**

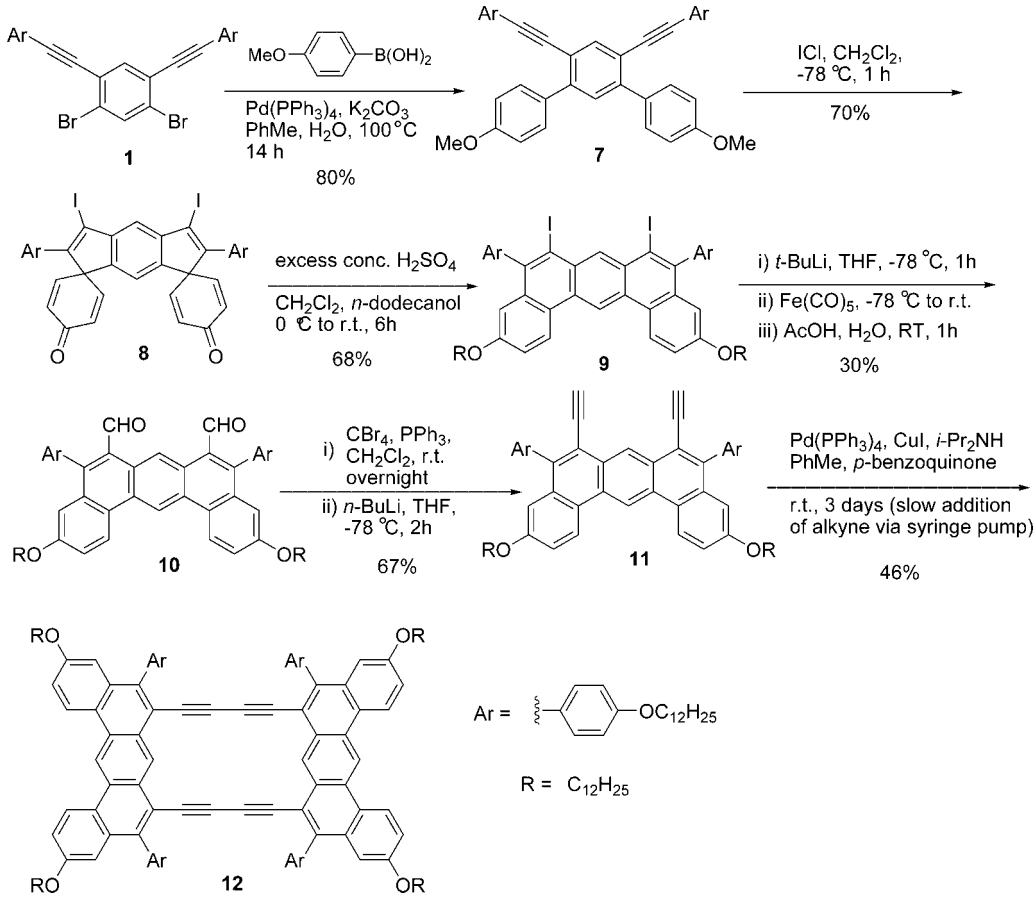

undefined mixtures. However, an indirect method involving a lithiation/carbonylation sequence to give **4**, followed by Corey−Fuchs homologation,[19] successfully afforded dialkyne **5**. Owing to the sterically encumbered environment of the reaction centers, dialdehyde **4** was always accompanied by the formation of monoaldehyde byproduct **13**. Separation of the two could however, be easily achieved by column chromatography. Finally, an oxidative coupling utilizing conditions previously developed[20] in our group was performed, furnishing macrocycles **6a** and **6b** in reasonable yields.

The synthesis of macrocycle **12** (Scheme 2) involved a similar sequence of transformations employed in the preparation of **6a** and **6b**, with the exception that the bis-alkoxyterphenyl **7** could only be converted to the desired diiodide **9** in two steps, via a skeletal rearrangement of the structurally intriguing **8**, using modifications of known reactions.[6,21] A second alkoxy-based macrocycle bearing branched farnesol-derived side chains was also synthesized in a manner analogous to **12**, with its existence confirmed by MALDI-TOF. Unfortunately, this fourth and final macrocycle could not be satisfactorily separated from a trimeric byproduct even after repeated column chromatography and attempted fractional recrystallizations. In addition to the three macrocycles, compound **15** (the acyclic analogue of **6a**) was also prepared to study the effect of the number of bridges on the photophysical properties. This was made in three steps (Scheme 3) starting from monoaldehyde **13**, which is a byproduct isolated during the purification of dialdehyde **4a**.

The above-mentioned target compounds were characterized by ^{1}H NMR, ^{13}C NMR, high-resolution mass spectrometry (MALDI-TOF), UV−vis, and fluorescence spectroscopy. In the ^{1}H NMR spectra of the macrocycles, the two protons located within the ring were found to be shifted downfield ($\delta \approx 9.5$ ppm) as a result of van der Waals deshielding brought about by steric interactions. The lack of any upfield shift of those internal protons implies the absence of a ring current[22] in these systems (i.e., no diatropic effect observed). Brief polarized optical microscopy experiments were also performed on the macrocycles in hope of finding liquid crystalline behavior as well, but the compounds had extremely high melting points (between 200 and 330 °C) and were also observed to decompose and discolor at those elevated temperatures.

Photophysical Studies. A SPEX fluorolog, with dual monochromators, was used to collect photoluminescence (PL) and photoluminescence excitation (PLE) spectra. The instrument is wavelength and intensity calibrated, and it compensates for variations in excitation intensity by monitoring the incident optical power level. In PL measurements, the **6a** films were optically excited at a wavelength $\lambda = 375$ nm. For PLE spectra,

(19) (a) Corey, E. J.; Fuchs, P. L. *Tetrahedron Lett.* **1972**, 3769–3772. (b) Ramirez, F.; Desai, N. B.; McKelvie, N. *J. Am. Chem. Soc.* **1962**, *84*, 1745–1747.
(20) Williams, V. E.; Swager, T. M. *J. Polym. Sci., Part A: Polym. Chem.* **2000**, *38*, 4669–4676.
(21) Li, C.-W.; Wang, C.-I.; Liao, H.-Y.; Chaudhuri, R.; Liu, R.-S. *J. Org. Chem.* **2007**, *72*, 9203–9207.
(22) (a) Fowler, P. W.; Lillington, M.; Olson, L. P. *Pure Appl. Chem.* **2007**, *79*, 969–980. (b) Boydston, A. J.; Haley, M. M.; Williams, R. V.; Armantrout, J. R. *J. Org. Chem.* **2002**, *67*, 8812–8819. (c) Soncini, A.; Domene, C.; Engelberts, J. J.; Fowler, P. W.; Rassat, A.; van Lenthe, J. H.; Havenith, R. W. A.; Jenneskens, L. W. *Chem.—Eur. J.* **2005**, *11*, 1257–1266. (d) Lepetit, C.; Godard, C.; Chauvin, R. *New J. Chem.* **2001**, *25*, 572–580.

Scheme 3. Synthesis of Acyclic **15**

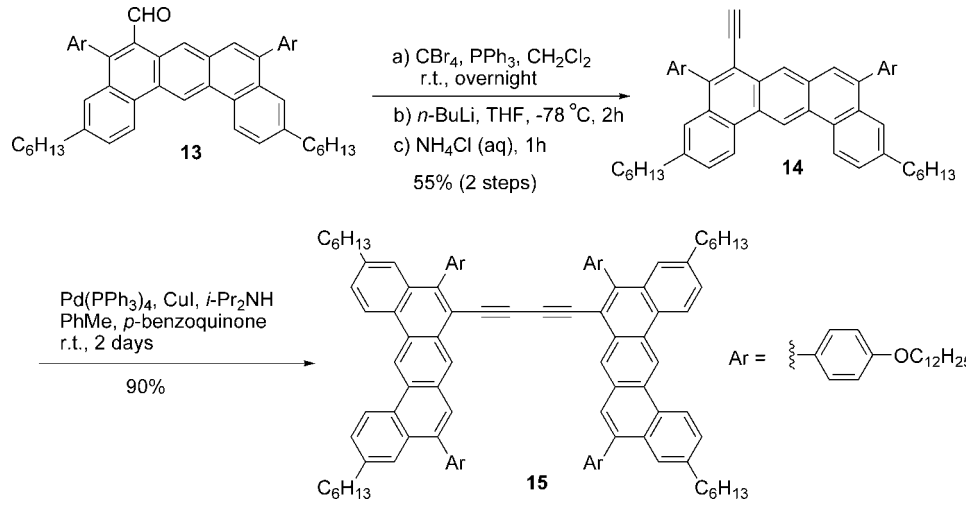

emission at $\lambda = 508$ nm was collected. Figure 1 shows the UV−vis absorption and fluorescence spectra of the four compounds in chloroform. Macrocycles **6a** and **6b** displayed essentially identical spectral profiles, with absorption and emission maxima occurring at around 440 and 455 nm, respectively. Changing the peripheral alkyl groups to alkoxy chains (e.g., **12**) resulted in a slight bathochromic shift, with the spectral shape remaining similar otherwise. The spectra of the acyclic **15** differed somewhat from the macrocycles, which was expected due to the major structural difference. Its absorption spectrum was blue-shifted relative to the others, possibly due to reduced conjugation resulting from the absence of the second diyne linker. A much larger Stokes shift was also observed, which could indicate reduced rigidity, once again as a result of having only a single linker. Fluorescence quantum yields of the compounds were measured against quinine sulfate in 0.1 N H_2SO_4 (Table 1). The three macrocycles in chloroform solution showed fairly high quantum yields between 0.40 and 0.50, whereas the singly bridged **15** had a lower value of 0.35.

To test for the presence of J-aggregates, we investigated the thin film photophysics of the macrocycles. As **6a** was synthesized in the largest quantity, films of this compound were studied in greatest detail. The initial films were produced by spin-coating a fairly concentrated (5 mg/mL) toluene solution of **6a** on to glass or quartz coverslips (18 × 18 mm^2). Fortuitously, the first few films showed promising UV−vis absorption features consistent with J-aggregates (Figure 2).

Table 1. Photophysical Properties of **6a**, **6b**, **12**, and **15**

compound	absorption max (nm)	emission max (nm)	quantum yield, Φ_F	extinction coefficient (M^{-1} cm^{-1})
6a	443	456	0.45	90141 (at 443 nm)
6b	443	456	0.43	63569 (at 443 nm)
12	448	461	0.47	79113 (at 448 nm)
15	395	440	0.35	38206 (at 395 nm)

Compared with the solution spectrum, the **6a** film spectrum shows an aggregate absorption peak at 467 nm (red-shifted by (23 ± 1) nm from the solution). Even more notable is the high intensity and narrow line width of this peak (J-band), which dominates all other spectral features. This is in stark contrast to the solution spectrum, in which the peak at 443 nm shows much lower intensity than those between 300 and 360 nm (absorptions due to pendant *p*-alkoxyphenyl moieties). Normalizing the solution and film absorbances at 340 nm, the enhancement in the peak intensity (at 467 nm) relative to the other spectral features becomes evident (Figure 2). The bathochromic shift and the strong intensity of the aggregate peak,

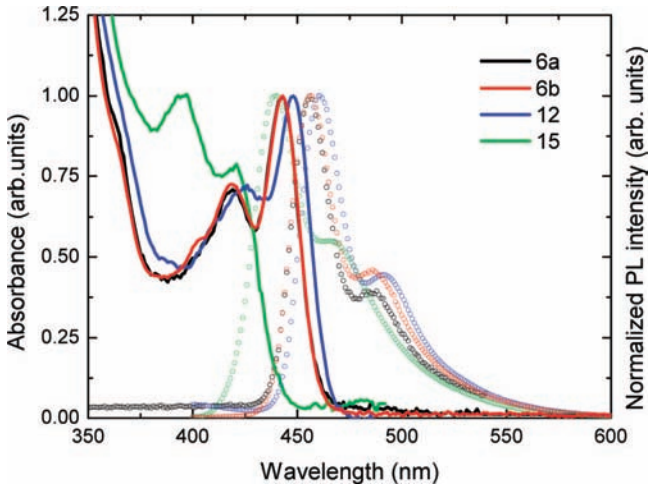

Figure 1. Normalized absorbance (solid lines) and emission (dotted lines) spectra of **6a**, **6b**, **12**, and **15** in chloroform.

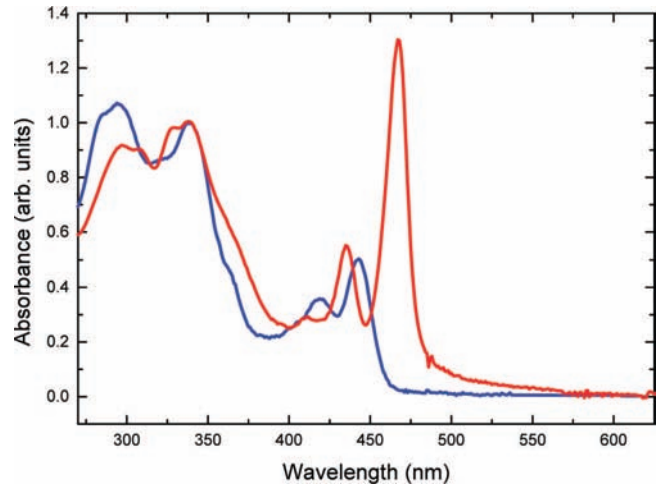

Figure 2. Absorption spectra of **6a**, solution (blue line) vs film (red line), normalized to the absorbance at 340 nm.

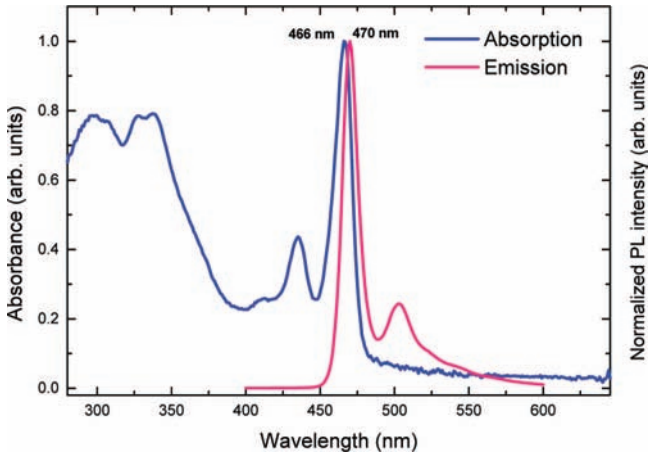

Figure 3. Normalized absorption (blue line) and fluorescence (pink line) spectra of **6a** (film).

are photophysical characteristics of J-aggregates.[23] From the emission spectra of the **6a** films we find the Stokes shift to be only 4 nm (Figure 3), versus 13 nm in solution phase. Such minimal Stokes shift is also consistent with the existence of J-aggregates.[24] It is notable that the fluorescence band is a mirror image of the low-energy edge of the J-band absorption.

We also find that it is possible to spin-coat films of **6a** that did not display a J-band. These less strongly absorbing films could be produced when the spin rate (of the spin-coating process) was high (e.g., 4000 rpm), a lower concentration (<2 mg/mL) of **6a** in solvent was used, or when a more volatile solvent (e.g., THF) was employed. The use of these parameters provided for less-than-favorable conditions for aggregate formation. However, when these 'nonaggregated' (i.e., monomeric) films were then subjected to conditions conducive to aggregate formation, the typical J-aggregate spectral features were found to emerge with time. This was achieved by vapor-annealing the films in a solvent chamber saturated with toluene vapor for 45 min, and then retrieving them for spectral (UV−vis) reacquisition. It can be seen (Figure 4) that the vapor-annealing, which should result in more ordered thin films,[25] precipitates the appearance of the highly intense J-band, confirming that molecular organization was indeed important in producing the desired J-aggregate photophysics. When the volatile THF is used as the spin-casting solvent (particularly with low **6a** concentration) the resulting films lacked J-aggregate features. However, J-aggregate features can be recovered when these films are placed in a solvent chamber containing THF vapor (Figure 4).

Similar photophysical experiments were also performed on films of the two longer-chained macrocyclic analogues **6b** and **12**. In both cases, the films are cast from THF solutions of the macrocycles and subsequently annealed under THF vapor for 45 min. UV−vis data are acquired before and after the annealing process, and the spectra of **6b** and **12** are shown in Figure 5. The spectra of the preannealed films did not show J-bands, but these appeared in both cases upon annealing. Therefore, the results obtained with **6b** and **12** were analogous to those of **6a**, suggesting that the doubling of chain length of the peripheral

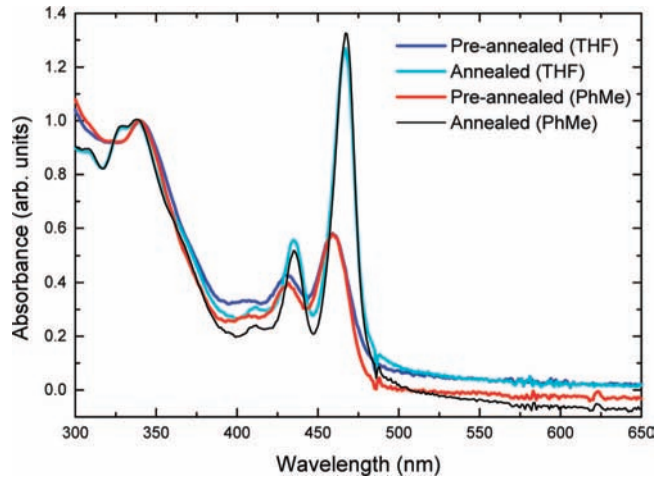

Figure 4. Absorption spectra of **6a** (film) before and after annealing under toluene (PhMe) and THF vapor, normalized to the absorbance at 340 nm.

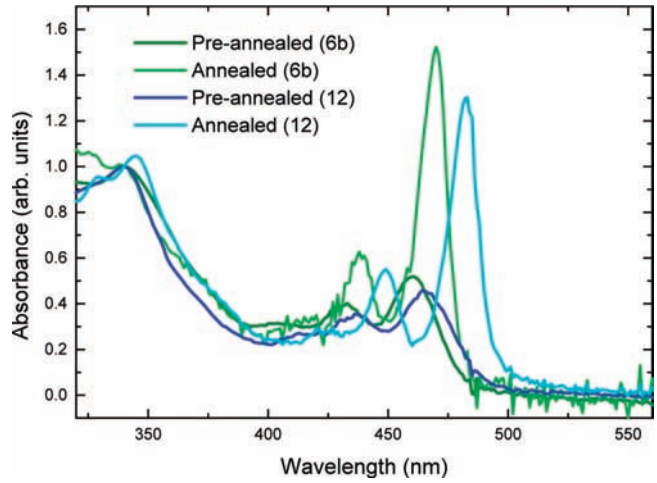

Figure 5. Absorption spectra of **6b** (film) and **12** (film) before and after annealing under THF vapor, normalized to the absorbance at 340 nm.

alkyl/alkoxy groups had little effect on the photophysics, be it in solution or in the film-state. Similar J-aggregate photophysics could not be observed with the noncyclic **15**, implying that the aggregate formation may require approximate molecular planarity (steric hindrance in the noncyclic **15** produces a larger deviation from planarity, since the two dibenzanthracene subunits are less constrained). It is likely that J-aggregation of these polycyclic aromatics in the solid-state relies on $\pi-\pi$ stacking interactions that could be disrupted if the nonplanarity became too pronounced.

Additional experiments examining the photophysics of **6a** as a function of concentration were also undertaken. A series of films were spin-coated using **6a** solutions (polyisobutylene matrix/chlorobenzene as solvent) of varying concentrations, and their photoluminescence spectra, excitation spectra, and fluorescence lifetimes were measured. Chlorobenzene was chosen as it provided for optimal comiscibility of **6a**, polyisobutylene, and solvent. When a film containing a very low concentration of **6a** (i.e., 0.0005 mg in a 1 mL solution of 40 mg/mL polyisobutylene (PIB) in chlorobenzene) was used, its emission peak was at 455 nm (Figure 6), identical to that observed in solution spectra. As the amount of **6a** used in the spin-coating process was increased to 0.002 mg/mL of PIB/chlorobenzene,

(23) (a) Jelley, E. E. *Nature (London)* **1936**, *138*, 1009. (b) Scheibe, G. *Angew. Chem.* **1936**, *49*, 563.
(24) Scheibe, G. *Optische Anregung organischer Systeme*, 2. Internationales Farbensymposium, Ed. Foerst, W., Verlag Chemie, Weinheim: 1966, p. 109.
(25) Mascaro, D. J.; Thompson, M. E.; Smith, H. I.; Bulović, V. *Org. Electron.* **2005**, *6*, 211–220.

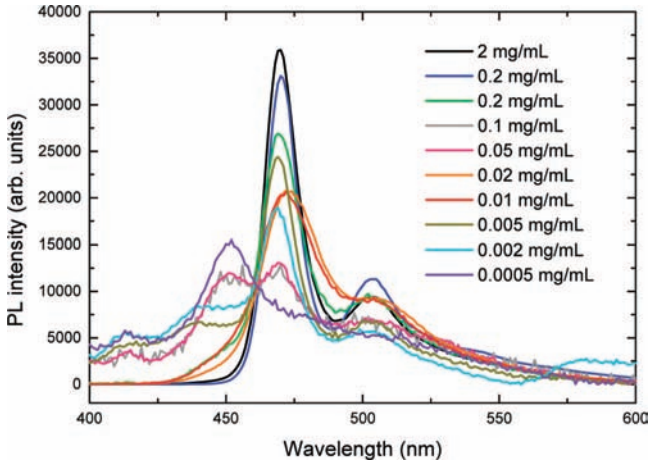

Figure 6. Photoluminescence intensity vs concentration of **6a** in thin films (PL scaled by subtracting the background and scaling by integrated intensity at all wavelengths).

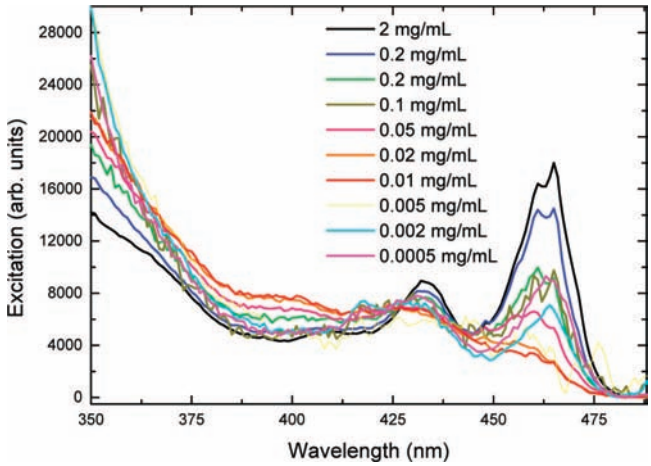

Figure 7. Excitation vs concentration of **6a** in thin films (PLE scaled by subtracting background and scaling by integrated intensity at all wavelengths).

aggregate peaks began to emerge at 470 nm with a shoulder at 500 nm, while the 455 nm "monomer" peak diminished. A further increase in **6a** concentration to 0.005 mg/mL resulted in further reduction in the 455 nm peak, so that at 0.02 mg/mL the monomer peak can no longer be observed, at which point the emission spectrum begins to resemble those obtained with neat films discussed above (pure **6a**, no PIB matrix). From the excitation spectra (Figure 7), no J-band at 470 nm could be observed at the lowest concentration of 0.0005 mg/mL, but as the concentration was increased 10-fold, a peak at 470 nm appeared, becoming more pronounced with increasing **6a** concentrations. Fluorescence lifetimes (at 470 nm) for a series of solutions and films of different concentrations were also measured. Solution lifetimes were found to be 1.7 ± 0.1 ns regardless of concentration. In the film state, it can be observed from Table 2 that the lifetimes generally decrease as the concentration of **6a** was increased from 0.0005 to 2.000 mg/mL (only a small incidence of scatter is observed in the trends). In particular, with a concentration of 0.0005 mg/mL, a lifetime of $\tau_m = 1.3$ ns was obtained, comparable to what was observed in chlorobenzene solutions, while at higher concentrations, lifetimes of about $\tau_J = 0.24$ ns are observed. Higher doping concentration also leads to a measurable increase in thin film photoluminescence (PL) quantum yield (QY) from $\Phi_m = 43\%$ ± 6% for the monomeric film to $\Phi_J = 92\%$ ± 8% for the aggregate films. To determine PL QY, we compared the PL counts from the **6a** film to a thin film standard of known QY, accounting for relative differences in absorption strength of the films. The standard was a thin film of thickness 75 nm of the small molecule tris-(8-hydroxyquinolinato)aluminum (Alq_3). The Alq_3 film was prepared by thermally evaporating recrystallized Alq_3 in ultra high vacuum (growth pressure below 10^{-6} Torr) onto a quartz substrate that was carefully solvent cleaned and oxygen plasma treated to remove trace impurities. The published QY for Alq_3 in thin film is 32% ± 2%.[26] We erred on the side of caution and used a value of QY = 30% for our calculations. To make a fair comparison of QY, for each film in consideration, the percentage of absorbed optical excitation was determined from optical transmission measurements. Measured PL counts were then normalized to the percent absorption values, on a film by film basis. For **6a** in monomeric form, we calculated the PL QY to be 43% ± 6%, which is similar to the QY for **6a** in solution, and for **6a** at high doping concentrations, we determined the QY to be 92% ± 8%.

Table 2. Fluorescence Lifetimes of **6a** (Solutions and Films) at Different Concentrations

concentration (mg/mL)	lifetimes (bimodal) (ns)		state
0.002	1.7 (100%)	–	solution (PhCl)
0.02	1.7 (100%)	–	solution (PhCl)
0.2	1.8 (100%)	–	solution (PhCl)
0.0005	1.3 (99.9%)	4.8 (0.1%)	film
0.002	0.2 (96.7%)	1.3 (3.3%)	film
0.005	0.3 (96.6%)	1.2 (3.4%)	film
0.01	0.3 (97.4%)	1.0 (2.6%)	film
0.02	0.2 (98.1%)	1.1 (1.9%)	film
0.05	0.6 (84.5%)	1.5 (15.5%)	film
0.10	0.4 (82.7%)	1.4 (17.3%)	film
0.20	0.4 (94.9%)	1.4 (5.1%)	film
2.00	0.2 (97.4%)	0.7 (2.6%)	film

The emergence of a red-shifted narrower line width optical transition at higher **6a** concentrations, the corresponding reduction in lifetime, and increase in quantum yield of aggregates as compared to monomers are indicative of J-aggregate formation.[27] In J-aggregates, strong coupling between the monomer transition dipoles produces a new cooperative molecular state. The coupling results in a new optical transition called the J-band, when the interaction strength exceeds the monomeric dephasing processes.[28] The interaction between monomeric transition dipoles lowers the overall energy of the cooperative state; hence, the J-band absorption/fluorescence is red-shifted relative to that of the monomer. In the J-aggregate state, multiple molecules coherently couple, the number being denoted by N_c, and the J-aggregate exciton delocalizes over all of them.[29] Coherent coupling among the N_c molecules leads to the acceleration of the radiative rate of the J-band states by a factor of N_c relative to the monomer,[30] which translates into shorter excited-state lifetime and higher PL QY. The radiative rate enhancement is typically referred to as a superradiance phenomenon since it is

(26) Garbuzov, D. Z.; Bulović, V.; Burrows, P. E.; Forrest, S. R. *Chem. Phys. Lett.* **1996**, *249*, 433–437.
(27) (a) Kuhn, H. *J. Chem. Phys.* **1970**, *53*, 101–108. (b) Kirstein, S.; Mohwald, H. *Adv. Mater.* **1995**, *7*, 460–463. (c) Peyratout, C.; Daehne, L. *Phys. Chem. Chem. Phys.* **2002**, *4*, 3032–3039.
(28) Spano, F. C.; Mukamel, S. *J. Chem. Phys.* **1989**, *91*, 683–700.
(29) Potma, E. O.; Wiersma, D. A. *J. Chem. Phys.* **1998**, *108*, 4894–4903.
(30) Vanburgel, M.; Wiersma, D. A.; Duppen, K. *J. Chem. Phys.* **1995**, *102*, 20–33.

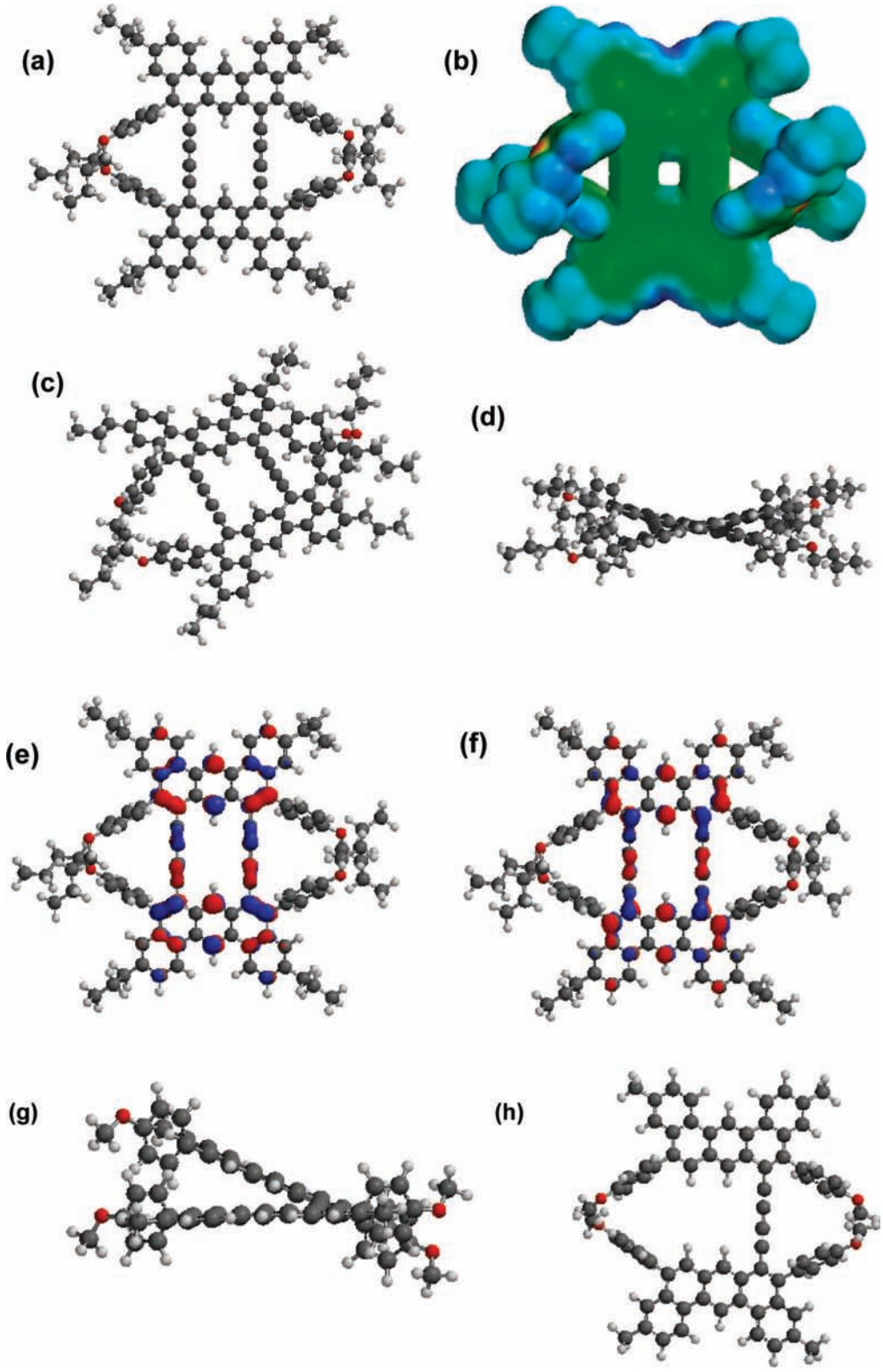

Figure 8. PM3-calculated models (a) top-down view of geometry-optimized macrocyclic structure, (b) molecular electrostatic potential map, (c) optimized structure tilted to emphasize steric crowding, (d) edge-on view of optimized structure, (e) frontier HOMO, (f) frontier LUMO, (g) edge-on view of the acyclic model structure, (h) and top-down view of the acyclic structure.

caused by coherent exciton coupling,[31] though in J-aggregates the mechanism for the coupling is near-field Coulombic interactions while in classic superradiant systems, the origin is interference effects in the spontaneous light emission process.[32] Since the radiative rate of a J-aggregate increases relative to that of the monomer by a factor of N_c, from a comparison of lifetimes (τ_J vs τ_m) and quantum yields (Φ_J vs Φ_m), N_c can be determined using the equation:[33]

$$N_c = \frac{\tau_m}{\tau_J}\frac{\Phi_J}{\Phi_m}$$

The data obtained suggest that N_c is on the order of 12 for our **6a** J-aggregate films. Coherent coupling also leads to a narrower total line width for the J-aggregate optical transition relative to the monomer because the delocalized exciton averages out site-to-site variations and suppresses the inhomogeneous broadening.[34] The linewidths of the monomer optical transition and the J-band are dominated by inhomogeneous broadening. Nevertheless, the width of the J-band relative to the monomer spectrum does characterize the coherence of the system. The line width of the J-band is narrower than the monomer optical transition because in the J-aggregate state, the exciton is delocalized over the N_c molecules that are coherently coupled, which tends to average out site-to-site inhomogeneities in the exciton energy. This motional narrowing is manifest in the smaller line width for J-aggregate absorption and emission spectra. This coherent coupling also results in the accelerated radiative process in the J-aggregate state, which translates into the higher observed QY and shorter exciton lifetime for the J-aggregate compared to the monomer.

Molecular Modeling. In order to better visualize the equilibrium geometry of the macrocycles **6a**, **6b**, and **12**, molecular calculations[35] were performed at the semiempirical PM3 level, using a model compound (Figure 8) with deliberately shortened alkyl side chains to enable more rapid completion of the calculation. As can be seen in Figure 8, the macrocycle is composed of two 1,3-butadiyne-linked planar dibenz[*a*,*j*]anthracene subunits that are slightly staggered relative to each other as a result of steric crowding in the middle of the molecule. Despite this structural distortion, the core of the macrocycle retains some overall planarity, which would still allow for intermolecular $\pi-\pi$ stacking interactions. By comparison, the acyclic analog shows greater nonplanarity (Figure 8g), since the two nonrestrained aromatic subunits have more freedom to minimize steric repulsions. As a result, $\pi-\pi$ stacking interactions in acyclic **15** may be weakened.

Conclusion

In summary, three dibenz[*a*,*j*]anthracene-based macrocycles have been synthesized and spectroscopically characterized. The conjugated macrocycles display pronounced photophysical properties in the solid state, such as the intense red-shifted absorbances, narrow linewidths, and small Stokes shifts, indicating J-aggregate formation. These new compounds may have the potential to be utilized in various optoelectronic devices (e.g., lasers, photovoltaics, and polaritonic devices[16a,36]).

Acknowledgment. This work was supported by the National Science Foundation and the Army Research Office's IED Stand-Off Detection Research Program (W911NF-07-1-0654), and the U.S. Army through the Institute for Soldier Nanotechnologies (DAAD-19-02-0002).

Supporting Information Available: Full experimental details pertaining to the synthesis of all new compounds described herein. This material is available free of charge via the Internet at http://pubs.acs.org.

JA900382R

(31) (a) Spano, F. C.; Kuklinski, J. R.; Mukamel, S. *Phys. Rev. Lett.* **1990**, *65*, 211–214. (b) De Boer, S.; Wiersma, D. A. *Chem. Phys. Lett.* **1990**, *165*, 45–53. (c) Spano, F. C.; Kuklinski, J. R.; Mukamel, S. *J. Chem. Phys.* **1991**, *94*, 7534–7544. (d) Meinardi, F.; Cerminara, M.; Sassella, A.; Bonifacio, R.; Tubino, R. *Phys. Rev. Lett.* **2003**, *91*, 247401.
(32) Dicke, R. H. *Phys. Rev.* **1954**, *93*, 99–110.
(33) Rousseau, E.; Van der Auweraer, M.; De Schryver, F. C. *Langmuir* **2000**, *16*, 8865–8870.
(34) Knapp, E. W.; Scherer, P. O. J.; Fischer, S. F. *Chem. Phys. Lett.* **1984**, *111*, 481–486.
(35) *Spartan '04 V1.0.0*; Wavefunction, Inc.: Irvine, CA; 2004.
(36) (a) Kena-Cohen, S.; Davanco, M.; Forrest, S. R. *Phys. Rev. Lett.* **2008**, *101*, 116401. (b) Holmes, R. J.; Forrest, S. R. *Phys. Rev. Lett.* **2004**, *93*, 186404. (c) Lidzey, D. G.; Bradley, D. D. C.; Skolnick, M. S.; Virgili, T.; Walker, S.; Whittaker, D. M. *Nature (London)* **1998**, *395*, 53–55.